Weierstraß-Institut
für Angewandte Analysis und Stochastik

im Forschungsverbund Berlin e. V.

Preprint ISSN 0946 – 8633

A posteriori optimization of parameters in stabilized methods for convection-diffusion problems — Part I

Volker John[1], Petr Knobloch[2], Simona B. Savescu[1]

submitted: July 16, 2010

[1] Weierstrass Institute for Applied Analysis and Stochastics, Mohrenstr. 39, 10117 Berlin, Germany
e-mail: Volker.John@wias-berlin.de
e-mail: Simona.B.Savescu@wias-berlin.de

[2] Charles University, Faculty of Mathematics and Physics, Department of Numerical Mathematics
Sokolovská 83, 186 75 Praha 8, Czech Republic
e-mail: knobloch@karlin.mff.cuni.cz

No. 1527
Berlin 2010

2010 *Mathematics Subject Classification.* 65N30.

Key words and phrases. Convection-diffusion problems, stabilized finite element methods, parameter optimization, SUPG method, residual-based error estimator.

Edited by
Weierstraß-Institut für Angewandte Analysis und Stochastik (WIAS)
Mohrenstraße 39
10117 Berlin
Germany

Fax: +49 30 2044975
E-Mail: preprint@wias-berlin.de
World Wide Web: http://www.wias-berlin.de/

Abstract

Stabilized finite element methods for convection-dominated problems require the choice of appropriate stabilization parameters. From numerical analysis, often only their asymptotic values are known. This paper presents a general framework for optimizing the stabilization parameters with respect to the minimization of a target functional. Exemplarily, this framework is applied to the SUPG finite element method and the minimization of a residual-based error estimator and error indicator. Benefits of the basic approach are shown and further improvements are discussed.

1 Introduction

The numerical solution of challenging problems in various engineering applications is in general not possible with standard methods that are based, e.g., on central finite differences or the Galerkin finite element method. More sophisticated schemes become necessary that are designed to tackle the special difficulties of the underlying problem.

An example, that will be considered in this paper, are scalar convection-dominated convection-diffusion equations. Solutions of these equations exhibit very fine structures, so-called layers, which cannot be resolved on meshes that are not extremely fine. Standard discretizations lead to solutions that are globally polluted by large spurious oscillations. In practice, stabilized methods are used. These methods introduce artificial diffusion. The difficulty consists now in defining the correct amount of diffusion at the correct positions in the correct directions (anisotropic diffusion) such that numerical solutions with sharp layers and without spurious oscillations are obtained. A method that is optimal with respect to all criteria does not exist yet. Many proposed stabilized methods include a so-called stabilization parameter (function) that usually has different values at different parts of the computational domain. Often, the asymptotic choice of the parameter is known, e.g., that it should be proportional to the local mesh width. However, in practice, the proportionality factor has to be chosen. There is the experience that different choices of such factors might lead to considerably different numerical solutions. Moreover, the asymptotic choice of the stabilization parameter is based on global stability and convergence analysis. Local features of solutions, like layers, are not taken into account in this analysis.

There should be mentioned a second example that demonstrates the difficulties of choosing parameters in numerical simulations – Large Eddy Simulation (LES) of turbulent flows. Turbulent flow simulations require the use of some turbulence model. An often used, so-called eddy viscosity model, is the Smagorinsky model [31]. This model is based on some insight into the physics of turbulent flows and it finally introduces a nonlinear viscosity into the discrete equations. It is rather easy to implement and very well understood from the point of view of mathematical analysis [27]. The derivation of the Smagorinsky model is based on some proportionality relations such that at the end a proportionality factor occurs. Experience shows that the use of a constant for this factor does not lead to good results. Instead, this factor has to be adapted to the local features of the flow field. An approach in this direction is the dynamic Smagorinsky model [8,28]. Despite all drawbacks, e.g., see [19], the dynamic Smagorinsky model is one of the most often used and most successful LES models. Nowadays, there is another approach to control the influence of the Smagorinsky model – Variational Multiscale (VMS) methods.

These methods try to select appropriate scales to which this model is applied [15,10,20,21]. Turbulent flow simulations are a typical example where principal forms of models are known but the results obtained with these models depend on the correct setting of parameters. There are many more numerical methods that require the choice of parameters and for which an a posteriori choice would greatly improve the ability to use them in applications. The a posteriori choice of parameters seems to be a widely open and challenging task in scientific computing.

The idea of choosing parameters in numerical methods a posteriori is not new, the dynamic Smagorinsky model was already mentioned. In essence, this method computes two discrete solutions in different ways and the parameter choice is based on comparing them. A method for hyperbolic conservation laws in one dimension can be found in [6]. In this paper, the streamline diffusion stabilization parameter and an adaptively refined grid are computed a posteriori. The adaptive algorithm uses the Dual Weighted Residual (DWR) approach, [1,2], with a backward-in-time dual problem. An iterative procedure based on equilibrating components of the error estimator is used to compute the stabilization parameter and the grids. The adaptive method led always to an improvement of the results compared with using a fixed stabilization parameter. This method was extended to one-dimensional nonlinear convection-diffusion-reaction equations in [13].

The present paper considers the Streamline-Upwind Petrov–Galerkin (SUPG) finite element method for scalar convection-dominated convection-diffusion equations introduced in [16,3]. Although a number of other stabilized finite element methods have been developed in the past decades, the SUPG method is still the standard approach. In essence, this method adds numerical diffusion in streamline direction. The amount of diffusion depends on local values of a stabilization parameter. There are different formulae for this parameter whose asymptotics are the same, see [22] for a discussion of parameter choices. The properties of solutions obtained with the SUPG method are well known: sharp layers at the correct positions are computed, but non-negligible spurious oscillations occur in a vicinity of layers. These oscillations make the use of the SUPG method in applications difficult as they correspond in general to unphysical situations, like negative concentrations. There have been a large number of attempts to improve the SUPG method in order to get rid of these oscillations while preserving its good properties. However, none of these so-called Spurious Oscillations at Layers Diminishing (SOLD) methods turned out to be entirely successful, [22,23].

To improve the solutions obtained with the SUPG method, the present paper pursues a different approach than the SOLD methods. It relies on the a posteriori optimization of the stabilization parameter, however, in contrast to [6,13], the parameter optimization is formulated as minimization of some functional, e.g., an a posteriori error estimator. This is a nonlinear constraint optimization problem that has to be solved iteratively. The key component of this approach consists in the efficient computation of the Fréchet derivative of the functional with respect to the stabilization parameter. This way utilizes an adjoint problem with an appropriate right-hand side. Concerning the topic of a posteriori parameter optimization, this paper presents a general approach and the consideration of the SUPG method is just an example of its application.

The paper is organized as follows. Section 2 presents the convection-diffusion problem under consideration and the SUPG method. A general approach of obtaining the Fréchet derivative of a functional that depends on the numerical solution with respect to parameters in the numerical method is presented in Section 3. This approach is applied to the SUPG method in Section 4. Section 5 contains a proof of concept. It is demonstrated that errors to known solutions can be reduced by using as functional to be minimized the error in some norm. For problems with unknown solutions, Section 6 illustrates the application of the a posteriori parameter choice based on the minimization of a residual-based a posteriori error estimator and error indicator. The most important conclusions and open problems are discussed in Section 7. Throughout the paper, standard notation is used for usual function spaces and norms, see, e.g., [4]. The notation $(\cdot,\cdot)_G$ with a set $G \subset \mathbb{R}^d$, $d = 1, 2, 3$, is used for the inner product in the space $L^2(G)$ or $L^2(G)^d$ and we set $(\cdot,\cdot) = (\cdot,\cdot)_\Omega$.

2 The convection-diffusion problem and its SUPG stabilization

Consider the scalar convection-diffusion problem

$$-\varepsilon\,\Delta u + \mathbf{b}\cdot\nabla u + c\,u = f \ \text{ in } \Omega, \qquad u = u_b \ \text{ on } \Gamma^D, \qquad \varepsilon\,\frac{\partial u}{\partial \mathbf{n}} = g \ \text{ on } \Gamma^N. \quad (1)$$

Here, $\Omega \subset \mathbb{R}^d$, $d = 2, 3$, is a bounded domain with a polyhedral Lipschitz–continuous boundary $\partial\Omega$ and Γ^D, Γ^N are disjoint and relatively open subsets of $\partial\Omega$ satisfying $\mathrm{meas}_{d-1}(\Gamma^D) > 0$ and $\overline{\Gamma^D \cup \Gamma^N} = \partial\Omega$. Furthermore, $\mathbf{n}$ is the outward unit normal vector to $\partial\Omega$, $\varepsilon > 0$ is a constant diffusivity, $\mathbf{b} \in W^{1,\infty}(\Omega)^d$ is the flow velocity, $c \in L^\infty(\Omega)$ is the reaction coefficient, $f \in L^2(\Omega)$ is a given outer source of the unknown scalar quantity u, and $u_b \in H^{1/2}(\Gamma^D)$, $g \in L^2(\Gamma^N)$ are given functions specifying the boundary conditions. The usual assumption that

$$c - \frac{1}{2}\,\mathrm{div}\,\mathbf{b} \geq c_0 \geq 0 \qquad (2)$$

with a constant c_0 is made. Moreover, it is assumed that

$$\{\mathbf{x} \in \partial\Omega\,;\ (\mathbf{b}\cdot\mathbf{n})(\mathbf{x}) < 0\} \subset \Gamma^D\,, \qquad (3)$$

i.e., the inflow boundary is a part of the Dirichlet boundary Γ^D.

This paper studies finite element methods for the numerical solution of (1). To this end, (1) is transformed into a variational formulation. Let $\widetilde{u}_b \in H^1(\Omega)$ be an extension of u_b (i.e., the trace of $\widetilde{u}_b$ equals u_b on Γ^D) and let

$$V = \left\{ v \in H^1(\Omega)\,;\ v = 0 \ \text{ on } \Gamma^D \right\} .$$

Then, a weak formulation of (1) reads: Find $u \in H^1(\Omega)$ such that $u - \widetilde{u}_b \in V$ and

$$a(u,v) = (f,v) + (g,v)_{\Gamma^N} \qquad \forall\ v \in V\,, \tag{4}$$

where

$$a(u,v) = \varepsilon\,(\nabla u, \nabla v) + (\mathbf{b}\cdot\nabla u, v) + (c\,u, v)\,.$$

In view of (2) and (3), the weak formulation (4) has a unique solution.

Let $\{\mathcal{T}_h\}_h$ be a family of triangulations of Ω parameterized by positive parameters h whose only accumulation point is zero. The triangulations $\mathcal{T}_h$ are assumed to consist of a finite number of open (mapped) polyhedral subsets K of Ω such that $\overline{\Omega} = \bigcup_{K\in\mathcal{T}_h} \overline{K}$ and the closures of any two different sets in $\mathcal{T}_h$ are either disjoint or possess either a common vertex or a common edge or (if $d = 3$) a common face. Further, it is assumed that any edge (face) of $\mathcal{T}_h$ which lies on $\partial\Omega$ is contained either in $\overline{\Gamma^D}$ or in $\overline{\Gamma^N}$.

For each h, a finite element space $W_h \subset H^1(\Omega)$ defined on $\mathcal{T}_h$ and approximating the space $H^1(\Omega)$ in the usual sense is introduced, see, e.g., [4]. Furthermore, for each h, let $\widetilde{u}_{bh} \in W_h$ be a function whose trace on Γ^D approximates u_b. Finally, we set $V_h = W_h \cap V$. Then, the Galerkin discretization of (1) reads: Find $u_h \in W_h$ such that $u_h - \widetilde{u}_{bh} \in V_h$ and

$$a(u_h, v_h) = (f, v_h) + (g, v_h)_{\Gamma^N} \qquad \forall\ v_h \in V_h\,. \tag{5}$$

Again, this problem is uniquely solvable. As discussed in the introduction, the Galerkin discretization (5) is inappropriate if convection dominates diffusion since in this case the discrete solution is usually globally polluted by spurious oscillations. An improvement can be achieved by adding a stabilization term to the Galerkin discretization. One of the most efficient procedures of this type is the SUPG method [16,3] that is frequently used because of its stability properties, its higher-order accuracy in appropriate norms and its easy implementation, see, e.g., [29].

The SUPG stabilization depends on a stabilization parameter that will be denoted by y_h in the following. It is assumed that all admissible stabilization parameters form a finite-dimensional space $Y_h \subset L^\infty(\Omega)$. For example, Y_h can consist of piecewise constant functions with respect to the triangulation $\mathcal{T}_h$.

The SUPG discretization of (1) reads: Find $u_h \in W_h$ such that $u_h - \widetilde{u}_{bh} \in V_h$ and

$$a(u_h, v_h) + s_h(y_h; u_h, v_h) = (f, v_h) + (g, v_h)_{\Gamma^N} + r_h(y_h; v_h) \qquad \forall\, v_h \in V_h\,, \quad (6)$$

where

$$\begin{aligned} s_h(y_h; u_h, v_h) &= (-\varepsilon\, \Delta_h u_h + \mathbf{b} \cdot \nabla u_h + c\, u_h, y_h\, \mathbf{b} \cdot \nabla v_h)\,, \\ r_h(y_h; v_h) &= (f, y_h\, \mathbf{b} \cdot \nabla v_h)\,. \end{aligned}$$

The SUPG method requires that the functions from W_h are H^2 on each mesh cell of $\mathcal{T}_h$, which is satisfied for common finite element spaces. The notation Δ_h denotes the Laplace operator defined cell-wise.

A detailed discussion of ways that are used in practice for choosing the stabilization parameter y_h in the case of first order finite elements can be found in [22]. Modifications for higher order finite elements are discussed, e.g., in [5,7]. A common choice is, for any mesh cell $K \in \mathcal{T}_h$,

$$y_h|_K = \frac{h_K}{2\, p\, |\mathbf{b}|}\, \xi(Pe_K) \quad \text{with} \quad \xi(\alpha) = \coth \alpha - \frac{1}{\alpha}\,, \quad Pe_K = \frac{|\mathbf{b}|\, h_K}{2\, p\, \varepsilon}\,, \quad (7)$$

where h_K is the cell diameter in the direction of the convection vector $\mathbf{b}$, p is the polynomial degree of the local finite element space, and Pe_K is the local Péclet number which determines whether the problem is locally (i.e., within a particular mesh cell) convection dominated or diffusion dominated. Note that, generally, the parameters h_K, Pe_K and $y_h|_K$ are functions of the points $\mathbf{x} \in K$. The evaluation of the cell diameter in the direction of the convection is discussed also in [22].

If (2) holds with $c_0 > 0$, a sufficient condition for the ellipticity of the bilinear form on the left-hand side of (6) in a standard SUPG norm is

$$0 \le y_h(\mathbf{x}) \le \frac{1}{2} \min \left\{ \frac{(\mathrm{diam}(K))^2}{\varepsilon\, c_{\mathrm{inv}}^2}, \frac{c_0}{\|c\|_{0,\infty,K}^2} \right\}, \quad \mathbf{x} \in K\,, \quad (8)$$

see [29], where $\mathrm{diam}(K)$ denotes the diameter of K, c_{inv} is a constant from the inverse inequality

$$\|\Delta v_h\|_{0,K} \le c_{\mathrm{inv}}\, [\mathrm{diam}(K)]^{-1}\, |v_h|_{1,K} \qquad \forall\, v_h \in V_h\,,$$

and $\|\cdot\|_{0,\infty,K}$ denotes the $L^\infty(K)$ norm. The first term in the minimum in (8) does not appear for P_1 finite elements and for Q_1 finite elements on rectangles since in these cases $\Delta_h v_h = 0$ for all $v_h \in V_h$.

An important class of convection-diffusion problems possesses the properties $\mathrm{div}\, \mathbf{b} = 0$, e.g., if $\mathbf{b}$ is the velocity field of an incompressible fluid, and $c = 0$.

Hence, (2) holds only with $c_0 = 0$. For this class of problems, one can prove the ellipticity of the SUPG bilinear form (in a weaker SUPG norm than for $c_0 > 0$) if

$$0 \le y_h(\mathbf{x}) \le \frac{(\mathrm{diam}(K))^2}{\varepsilon\, c_{\mathrm{inv}}^2}, \quad \mathbf{x} \in K\,. \tag{9}$$

For the same reason as above, the bound on the right-hand side of (9) is not needed if P_1 finite elements or Q_1 finite elements on rectangles are used.

In the special case of a constant convection field and a uniform grid, the stabilization parameter given by (7) is the same in all mesh cells, independently of local features of the solution, like layers. This does not seem to be an optimal choice. This paper will present and study an approach to choose the values of the stabilization parameter locally, based on the minimization of a functional that measures or estimates the accuracy of the computed solution.

3 Optimization of parameters in numerical methods with respect to the minimization of a functional

Let us assume that a numerical method for the solution of (1) is given and let the method depend on a parameter $y_h \in Y_h$. An example is the SUPG method (6). Let $D_h \subset Y_h$ be an open set such that, for any $y_h \in D_h$, the considered method has a unique solution $u_h \in W_h$. To emphasize that u_h depends on y_h, we shall write $u_h(y_h)$ instead of u_h in the following. Let $I_h : W_h \to \mathbb{R}$ be a functional such that

$$\Phi_h(y_h) := I_h(u_h(y_h))$$

represents a measure of the error of the discrete solution $u_h(y_h)$ corresponding to a given parameter y_h. The aim is to compute a parameter $y_h \in D_h$ for which Φ_h attains a minimum on D_h or is near to a minimum (or the infimum) of Φ_h on D_h. This nonlinear minimization problem has to be solved iteratively. Reasonable iterative schemes require at least information on how Φ_h changes if the parameter y_h is changed, i.e., on the Fréchet derivative of Φ_h. An efficient way to compute this derivative is needed. Such a way will be explained in this section.

For any $y_h \in D_h$, it holds $u_h(y_h) = \widetilde{u}_h(y_h) + \widetilde{u}_{bh}$ with $\widetilde{u}_h : D_h \to V_h$. Thus, one does not need to consider the space W_h in the optimization process but can work with the space V_h, which is more convenient.

Denote $\tilde{I}_h(w_h) = I_h(w_h + \widetilde{u}_{bh})$ for any $w_h \in V_h$. Then $\tilde{I}_h : V_h \to \mathbb{R}$ and

$$\Phi_h(y_h) = \tilde{I}_h(\widetilde{u}_h(y_h)) \qquad \forall\ y_h \in D_h\,.$$

Let us assume that the mappings $\tilde{I}_h = \tilde{I}_h(w_h)$ and $\widetilde{u}_h = \widetilde{u}_h(y_h)$ are Fréchet–

differentiable. The Fréchet derivatives are denoted by $D\tilde{I}_h : V_h \to V_h'$ and $D\widetilde{u}_h : D_h \to \mathcal{L}(Y_h, V_h)$. Then, the Fréchet derivative $D\Phi_h : D_h \to Y_h'$ of Φ_h exists and is given by

$$D\Phi_h(y_h) = D\tilde{I}_h(\widetilde{u}_h(y_h))D\widetilde{u}_h(y_h) \quad \forall\, y_h \in D_h. \tag{10}$$

The naive way of using this formula for computing $D\Phi_h(y_h)$ is very inefficient as the computation of $D\widetilde{u}_h(y_h)$ requires the solution of $\dim Y_h$ systems of $\dim V_h$ algebraic equations.

The problem of efficiently evaluating a derivative of form (10) is well known, e.g., from optimal control of partial differential equations. There is a way for obtaining this derivative that is based on an appropriate adjoint problem, e.g., see [33]. This way will be applied to the situation considered in this paper. The minimization of Φ_h occurs under the condition that $u_h(y_h)$ should fulfill the discretized partial differential equation (6), i.e., for a residual operator $R_h : V_h \times Y_h \to V_h'$ holds

$$R_h(\widetilde{u}_h(y_h), y_h) = 0 \qquad \forall\, y_h \in D_h\,. \tag{11}$$

For the SUPG method (6), the operator R_h is given by

$$\begin{aligned}\langle R_h(w_h, y_h), v_h\rangle = {} & a(w_h + \widetilde{u}_{bh}, v_h) + s_h(y_h; w_h + \widetilde{u}_{bh}, v_h) - (f, v_h)\\ & -(g, v_h)_{\Gamma^N} - r_h(y_h; v_h) \qquad \forall\, v_h, w_h \in V_h, y_h \in Y_h\,.\end{aligned}$$

Differentiating (11) with respect to y_h leads to

$$\partial_w R_h(\widetilde{u}_h(y_h), y_h)D\widetilde{u}_h(y_h) + \partial_y R_h(\widetilde{u}_h(y_h), y_h) = 0 \quad \forall\, y_h \in D_h, \tag{12}$$

provided that the mapping $R_h = R_h(w_h, y_h)$ is Fréchet–differentiable. Note that $\partial_w R_h : V_h \times Y_h \to \mathcal{L}(V_h, V_h')$ and $\partial_y R_h : V_h \times Y_h \to \mathcal{L}(Y_h, V_h')$. Assume that there is a mapping $\psi_h : D_h \to V_h$ such that

$$\langle D\Phi_h(y_h), \tilde{y}_h\rangle = -\langle(\partial_y R_h)(\widetilde{u}_h(y_h), y_h)\tilde{y}_h, \psi_h(y_h)\rangle \qquad \forall\, y_h \in D_h,\ \tilde{y}_h \in Y_h\,. \tag{13}$$

Then, according to (12), one obtains

$$\begin{aligned}&\langle D\Phi_h(y_h), \tilde{y}_h\rangle\\ &= \langle(\partial_w R_h)(\widetilde{u}_h(y_h), y_h)D\widetilde{u}_h(y_h)\tilde{y}_h, \psi_h(y_h)\rangle\\ &= \langle(\partial_w R_h)'(\widetilde{u}_h(y_h), y_h)\psi_h(y_h), D\widetilde{u}_h(y_h)\tilde{y}_h\rangle \qquad \forall\, y_h \in D_h,\ \tilde{y}_h \in Y_h\,,\end{aligned}$$

where the adjoint operator is defined by

$$\langle(\partial_w R_h)'(w_h, y_h)v_h, \tilde{v}_h\rangle = \langle(\partial_w R_h)(w_h, y_h)\tilde{v}_h, v_h\rangle \quad \forall\, v_h, \tilde{v}_h, w_h \in V_h, y_h \in Y_h\,.$$

On the other hand, from (10) follows that

$$
\begin{aligned}
\langle D\Phi_h(y_h), \tilde{y}_h\rangle &= \langle D\tilde{I}_h(\widetilde{u}_h(y_h))D\widetilde{u}_h(y_h), \tilde{y}_h\rangle \\
&= \langle D\tilde{I}_h(\widetilde{u}_h(y_h)), D\widetilde{u}_h(y_h)\tilde{y}_h\rangle \qquad \forall\, y_h \in D_h\,, \tilde{y}_h \in Y_h\,.
\end{aligned}
$$

The two representations of $D\Phi_h(y_h)$ suggest to define $\psi_h(y_h)$ as the solution of the adjoint problem, cf., e.g., [9,30],

$$
(\partial_w R_h)'(\widetilde{u}_h(y_h), y_h)\, \psi_h(y_h) = D\tilde{I}_h(\widetilde{u}_h(y_h)) \qquad \forall\, y_h \in D_h. \tag{14}
$$

Then ψ_h satisfies (13) and hence the Fréchet derivative of Φ_h is given by

$$
D\Phi_h(y_h) = -(\partial_y R_h)'(\widetilde{u}_h(y_h), y_h)\psi_h(y_h) \qquad \forall\, y_h \in D_h. \tag{15}
$$

The adjoint operator is defined by

$$
\langle(\partial_y R_h)'(w_h, y_h)v_h, \tilde{y}_h\rangle = \langle(\partial_y R_h)(w_h, y_h)\tilde{y}_h, v_h\rangle \quad \forall\, v_h, w_h \in V_h, y_h, \tilde{y}_h \in Y_h\,.
$$

To clarify the approach, we would like to give its algebraic version. All operators and functionals are defined using finite-dimensional spaces, such that their Fréchet derivatives can be represented by matrices and vectors. Let $y_h \in D_h$ be given and let us denote by $D\Phi_h \in \mathbb{R}^{1\times \dim Y_h}$ and $D\tilde{I}_h \in \mathbb{R}^{1\times \dim V_h}$ the vectors representing the derivatives $D\Phi_h(y_h)$ and $D\tilde{I}_h(\widetilde{u}_h(y_h))$, respectively. Furthermore, we denote by $D\widetilde{u}_h \in \mathbb{R}^{\dim V_h \times \dim Y_h}$, $\partial_w R_h \in \mathbb{R}^{\dim V_h \times \dim V_h}$, and $\partial_y R_h \in \mathbb{R}^{\dim V_h \times \dim Y_h}$ the matrices representing the derivatives $D\widetilde{u}_h(y_h)$, $\partial_w R_h(\widetilde{u}_h(y_h), y_h)$, and $\partial_y R_h(\widetilde{u}_h(y_h), y_h)$, respectively. Then, equation (10) holds true if and only if

$$
D\Phi_h \mathbf{y} = D\tilde{I}_h D\widetilde{u}_h \mathbf{y} \quad \forall\, \mathbf{y} \in \mathbb{R}^{\dim Y_h}. \tag{16}
$$

Relation (12) is equivalent to

$$
\mathbf{v}^T \partial_w R_h D\widetilde{u}_h \mathbf{y} = -\mathbf{v}^T \partial_y R_h \mathbf{y} \quad \forall\, \mathbf{v} \in \mathbb{R}^{\dim V_h}. \tag{17}
$$

The goal of the adjoint approach consists in reformulating the right-hand side of (16). To this end, choose $\mathbf{v}$ in (17) such that $\mathbf{v}^T \partial_w R_h = D\tilde{I}_h$, i.e.,

$$
\boldsymbol{\psi} := \mathbf{v} = (\partial_w R_h)^{-T} D\tilde{I}_h^T,
$$

which is the algebraic version of (14). Inserting $\boldsymbol{\psi}$ into (16) and using (17) gives

$$
D\Phi_h \mathbf{y} = \boldsymbol{\psi}^T \partial_w R_h D\widetilde{u}_h \mathbf{y} = -\boldsymbol{\psi}^T \partial_y R_h \mathbf{y} \quad \forall\, \mathbf{y} \in \mathbb{R}^{\dim Y_h}.
$$

This is equivalent to

$$
D\Phi_h = -\boldsymbol{\psi}^T\, \partial_y R_h,
$$

that is the algebraic version of (15).

4 Application to the SUPG method

For the SUPG method (6), there is

$$\begin{aligned}\langle (\partial_w R_h)(w_h, y_h)\tilde{v}_h, v_h\rangle &= a(\tilde{v}_h, v_h) + s_h(y_h; \tilde{v}_h, v_h)\,,\\ \langle (\partial_y R_h)(w_h, y_h)\tilde{y}_h, v_h\rangle &= s_h(\tilde{y}_h; w_h + \tilde{u}_{bh}, v_h) - r_h(\tilde{y}_h; v_h)\end{aligned}$$

for any $y_h, \tilde{y}_h \in D_h$ and $v_h, \tilde{v}_h, w_h \in V_h$. Thus, for any $y_h \in Y_h$, the auxiliary function $\psi_h(y_h) \in V_h$ is the solution of

$$a(v_h, \psi_h(y_h)) + s_h(y_h; v_h, \psi_h(y_h)) = \langle D\tilde{I}_h(\tilde{u}_h(y_h)), v_h\rangle \qquad \forall\ v_h \in V_h \qquad (18)$$

and the Fréchet derivative of Φ_h is given by

$$\langle D\Phi_h(y_h), \tilde{y}_h\rangle = -s_h(\tilde{y}_h; u_h(y_h), \psi_h(y_h)) + r_h(\tilde{y}_h; \psi_h(y_h)) \qquad \forall\ \tilde{y}_h \in Y_h\,.$$

We define Y_h as the space of piecewise constant functions. After having solved (18) for a given stabilization parameter y_h, the Fréchet derivative of Φ_h at y_h with respect to the stabilization parameter is available. A straightforward idea for the solution of the nonlinear minimization problem consists in applying a damped steepest descent method. Let $y_h^{(k)}$ be a given stabilization parameter, then the iteration has the form

$$y_h^{(k+1)} = y_h^{(k)} - \alpha^{(k)} D\Phi_h\left(y_h^{(k)}\right), \quad k = 0, 1, 2, \ldots, \qquad (19)$$

where $\alpha^{(k)}$ is a damping parameter.

The efficiency of the iteration depends of course on the choice of the damping parameters. In our implementation of the method, the decrease of the functional Φ_h will be locally maximized. To this end, the initial guess for each damping factor $\alpha^{(k)}$ is a value α_{ini}. If the application of α_{ini} leads to a reduction of the target functional, the damping factor will be doubled. This step is repeated as long as the target functional decreases. If the application of α_{ini} does not lead to a reduction of the value of the target functional, α_{ini} will be divided by 2. The reduction of α_{ini} will be stopped if either a damping parameter is found that leads to a decrease of Φ_h or if a minimal value $\alpha_{\min}$ for the damping factor is obtained. The iteration stops either after reaching a prescribed maximal number of iterations $k_{\max}$, or after the damping parameter becomes less than $\alpha_{\min}$, or if the decrease of the target functional becomes too slow. The concrete test for the last stopping criterion is

$$\frac{\Phi_h\left(y_h^{(k-10)}\right) - \Phi_h\left(y_h^{(k)}\right)}{\Phi_h\left(y_h^{(k-10)}\right)} \le d_{\min}, \quad k \ge 10.$$

Of course, before the solution with a proposed new parameter $y_h^{(k+1)}$ is computed, the stabilization parameter is always restricted to admissible values given by (8) or (9). The values from [12] are used for c_{inv} in (8) and (9). If not mentioned otherwise, the stabilization parameter was initialized with the standard choice (7).

5 Proof of concept: parameter optimization with respect to errors

A common approach for supporting error estimates consists in prescribing a solution of (1), that defines also the right-hand side and the boundary conditions of (1), and measuring errors in certain norms of the numerical solution. If errors can be measured, it should be possible with the proposed methodology to compute the SUPG stabilization parameter such that these errors are reduced compared with the standard choice of the SUPG parameter (7). This section studies this topic.

Numerical studies with respect to the error in the $L^2(\Omega)$ norm and the $H^1(\Omega)$ seminorm were performed. For shortness, the detailed presentation will be restricted to the error in the $L^2(\Omega)$ norm

$$I_h(w_h) = \|u - w_h\|_{0,\Omega}^2. \tag{20}$$

Then, the right-hand side of the adjoint problem (14) becomes

$$\langle D\tilde{I}_h(\tilde{u}_h(y_h)), v_h\rangle = -2(u - u_h(y_h), v_h).$$

At the end of this section, some remarks will be given on the parameter optimization with respect to the error in the $H^1(\Omega)$ seminorm.

A difficulty consists in finding or defining examples that on the one hand have a known solution and on the other hand possess typical features of solutions of convection-dominated problems, in particular layers. Below, results obtained with two examples defined in [25] will be presented. The solutions of these examples depend on the diffusion coefficient ε, and so the right-hand sides do. As already noticed in [26], high order quadrature rules are necessary to keep the quadrature error for the right-hand side small for small ε. For this reason, the diffusion parameter was chosen only three or four orders of magnitude smaller than the convection in these examples.

Both examples are defined on the unit square. In the computations, triangular grids (Grid 1 in Fig. 1) with P_1, P_2, P_3 finite elements and square grids (Grid 2) with Q_1, Q_2, Q_3 finite elements were used. Level 0 of Grid 1 consists of two triangles and level 0 of Grid 2 of one square. The grids were regularly refined using so-called red refinement. A quadrature rule that is exact for polynomials of degree 19 was used on triangles and a Gaussian quadrature rule that is exact for polynomials of degree 17 on squares.

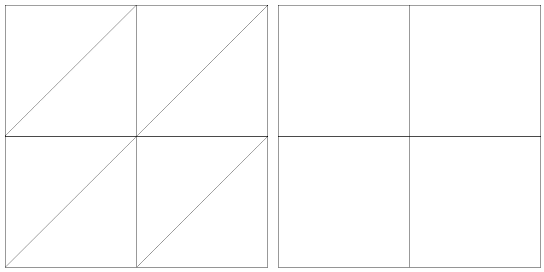

Fig. 1. Types of triangulations used in the computations: Grid 1 and Grid 2 (level 1).

In the iteration (19), the initial damping parameter was set to $\alpha_{\text{ini}} = 10^{-6}$, the minimal damping parameter to $\alpha_{\min} = 10^{-12}$, the maximal number of iterations to $k_{\max} = 100000$ (which was never reached) and $d_{\min} = 10^{-4}$. The computations were performed with code MooNMD [24]. The implementation was double-checked at selected examples with a second code.

Example 5.1 *Example with interior layer.* This example is given by $\Omega = (0,1)^2$, $\varepsilon = 10^{-4}$, $\mathbf{b} = (2,3)$, $c = 2$, and the right-hand side and the Dirichlet boundary condition on $\Gamma^D = \partial\Omega$ are prescribed such that

$$\begin{aligned} u(x,y) &= 16x(1-x)y(1-y) \\ &\quad \times \left(\frac{1}{2} + \frac{\arctan[2\varepsilon^{-1/2}(0.25^2 - (x-0.5)^2 - (y-0.5)^2)]}{\pi} \right) \end{aligned}$$

is the solution of (1).

A comparison of the $L^2(\Omega)$ errors obtained with the standard parameter choice (7) and the a posteriori choice based on I_h defined by (20) is presented in Fig. 2. It can be observed that the a posteriori parameter choice leads in fact to solutions with smaller $L^2(\Omega)$ error. However, for the third order finite element, the error reduction is very small. Particularly on the finer grids, the layers are resolved and the stabilization has little influence. Since the convection is constant, the standard parameter (7) is constant on a given grid, too. Fig. 3 shows the a posteriori computed stabilization parameter for different finite elements on a certain grid level. The corresponding standard parameters are given in the caption. It can be seen that the a posteriori methodology changes the parameter in the layer. There is not only an increase compared with the standard parameter. In some mesh cells, the parameter is reduced and sometimes even set to zero. A large stabilization parameter can be observed at the front and the back (with respect to the direction of the convection) of the body. Visually, the computed solutions look more or less the same.

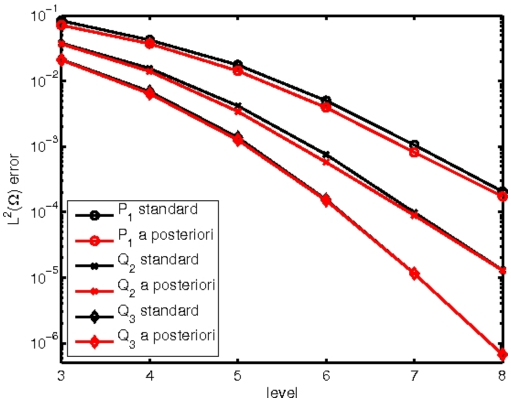

Fig. 2. Example 5.1, $L^2(\Omega)$ errors for different finite elements, comparison of standard parameter choice (7) and the a posteriori choice based on minimizing the $L^2(\Omega)$ error.

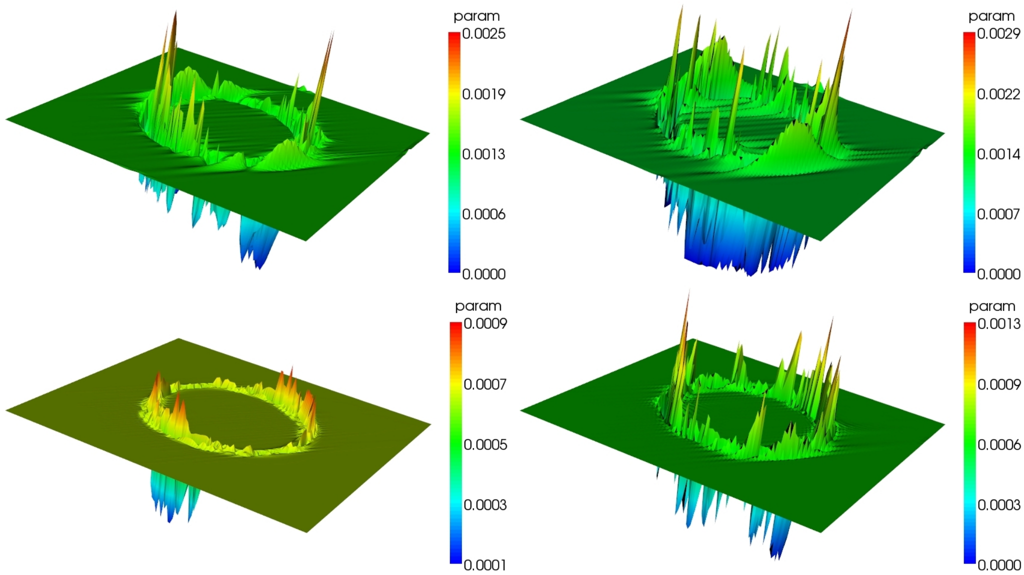

Fig. 3. Example 5.1, a posteriori computed stabilization parameters; top left: P_1, standard parameter $y_h = 1.294391e-3$; top right: Q_1, standard parameter $y_h = 1.294391e-3$; bottom left: P_2, standard parameter $y_h = 6.433494e-4$; bottom right: Q_2, standard parameter $y_h = 6.433494e-4$; all level 7.

Example 5.2 *Example with boundary layer.* This example is defined by $\Omega = (0,1)^2$, $\varepsilon = 10^{-3}$, $\mathbf{b} = (2,3)$, and $c = 1$. The prescribed solution

$$
\begin{aligned}
u(x,y) = {} & xy^2 - y^2 \exp\left(\frac{2(x-1)}{\varepsilon}\right) - x \exp\left(\frac{3(y-1)}{\varepsilon}\right) \\
& + \exp\left(\frac{2(x-1)+3(y-1)}{\varepsilon}\right)
\end{aligned}
$$

defines the right-hand side and the Dirichlet boundary condition on $\Gamma^D = \partial\Omega$.

Fig. 4 presents comparisons of the $L^2(\Omega)$ errors obtained with the standard and the a posteriori parameter choices. Clearly, the a posteriori parameter choice leads always to a reduction of the $L^2(\Omega)$ errors. However, a higher order of convergence cannot be observed. The a posteriori computed parameters are presented in Fig. 5. It can be observed that the optimization of the $L^2(\Omega)$ error reduces the stabilization parameter in the layers.

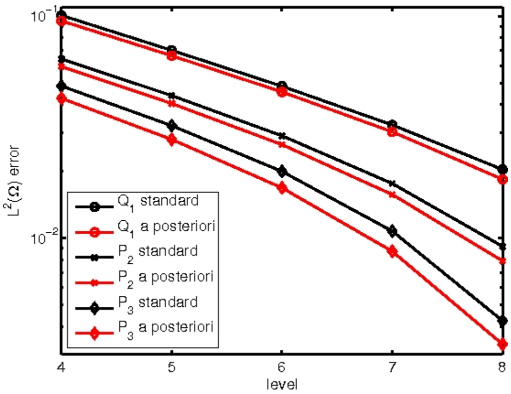

Fig. 4. Example 5.2, $L^2(\Omega)$ errors for different finite elements, comparison of standard parameter choice (7) and the a posteriori choice based on minimizing $L^2(\Omega)$ error.

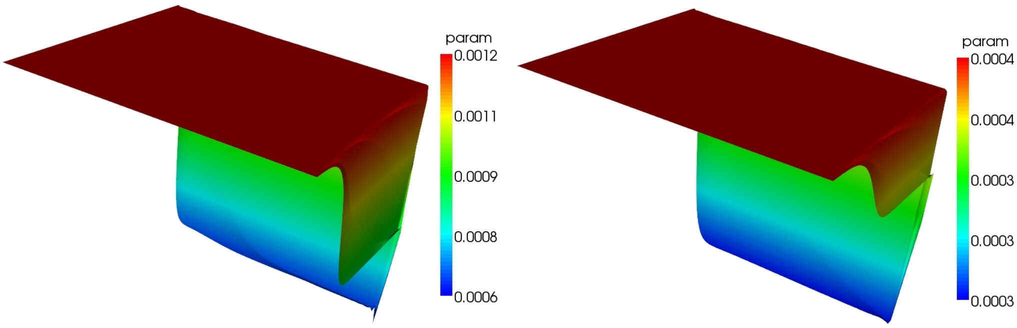

Fig. 5. Example 5.2, a posteriori computed stabilization parameters; left: Q_1, standard parameter $y_h = 1.225160e-3$; right: Q_2, standard parameter $y_h = 5.741186e-4$; all level 7.

Concerning the a posteriori parameter choice based on the error in the $H^1(\Omega)$ seminorm, we could observe essentially the same behavior as for the $L^2(\Omega)$ norm: the $H^1(\Omega)$ seminorm error becomes always smaller than for the solution with the standard parameter (7). However, sometimes the error reduction is very small. Because of the unresolved layers, in particular in Example 5.2, the error in the $H^1(\Omega)$ seminorm grows on coarse grids, compare Fig. 6, left picture.

Considering all three parameter choices (standard, a posteriori based on $L^2(\Omega)$ error, a posteriori based on $H^1(\Omega)$ seminorm error) one can observe that the optimization with respect to the error in one norm might reduce the error in the other norm, too, compared with the standard parameter choice. But the other error might also increase, see Fig. 6. Fig. 7 presents stabilization parameters and corresponding solutions with respect to the minimization of errors in different norms. Whereas the minimization of the $L^2(\Omega)$ error reduces the parameter in the boundary layers, the minimization with respect to the error in the $H^1(\Omega)$ seminorm increases it in the layer at $x = 1$. The different effects on the computed solutions are clearly visible. In the $L^2(\Omega)$ error optimized solution, spurious oscillations can be observed in the layers. They are even larger than with the standard parameter (7). The computed solution with $H^1(\Omega)$ seminorm error minimization looks much better. This comparison demonstrates the importance of using an appropriate measure on which the a posteriori selection of the stabilization parameter is based.

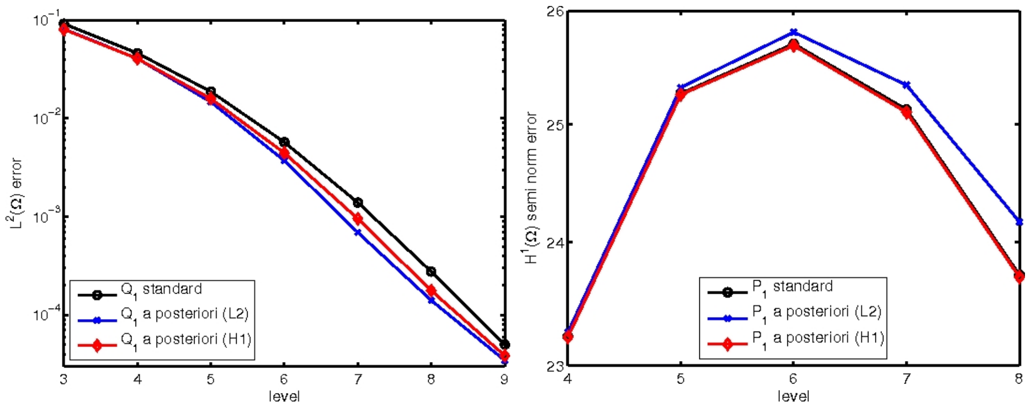

Fig. 6. Left: Example 5.1, Q_1 finite element and $L^2(\Omega)$ error; right: Example 5.2, P_1 finite element and $H^1(\Omega)$ seminorm error; comparison of the different parameter choices.

Altogether, the results presented in this section demonstrate that the proposed methodology is able to obtain a stabilization parameter in the SUPG method in an a posteriori way such that solutions with reduced errors are obtained.

6 Parameter optimization with respect to an error estimator and an error indicator

Generally, the evaluation of errors is not possible as the solution of (1) is not known. In this situation, other functionals are necessary to measure or estimate the accuracy of computed solutions. A posteriori error estimators are the appropriate tool.

The construction of reliable error estimators with respect to global norms for convection-dominated problems is a difficult problem. As demonstrated, e.g., in [18], the application of standard estimators for elliptic problems does not lead to reliable error predictions. The numerical studies will consider a residual-based error estimator from [34]

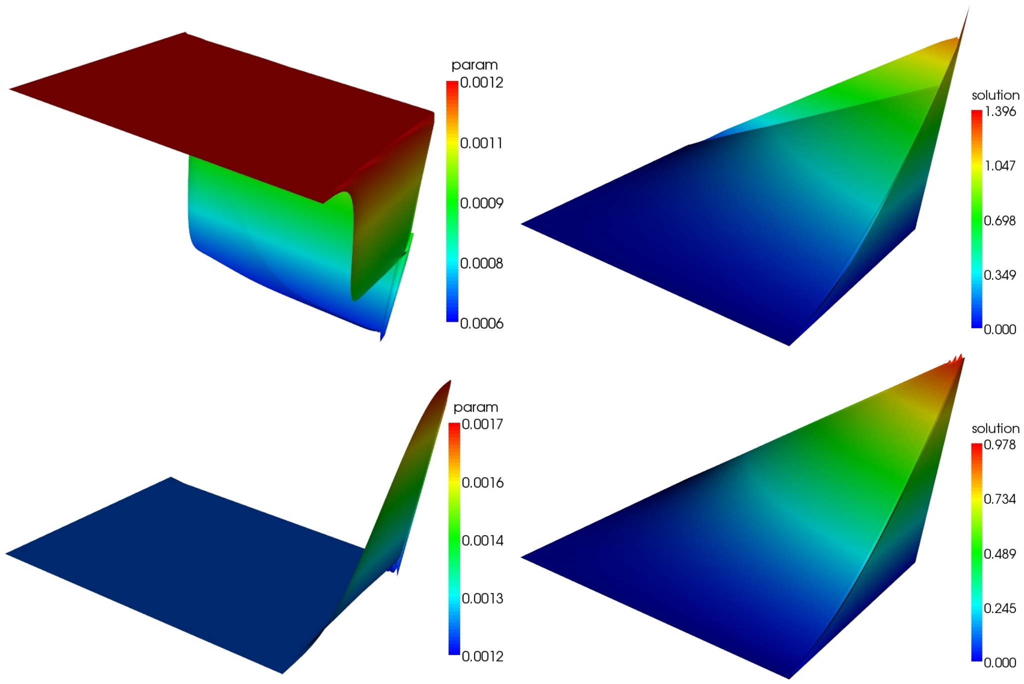

Fig. 7. Example 5.2, a posteriori computed stabilization parameters and computed solutions with the P_1 finite element; top: optimization with respect to the $L^2(\Omega)$ error; bottom: optimization with respect to the $H^1(\Omega)$ seminorm error; both at level 7.

$$I_h(w_h) = \sum_{K\in\mathcal{T}_h} \alpha_K^2 \, \| -\varepsilon\,\Delta w_h + \mathbf{b}\cdot\nabla w_h + c\,w_h - f\|_{0,K}^2 + \sum_{E\subset\partial K} \varepsilon^{-1/2}\alpha_E \|R_E(w_h)\|_{0,E}^2 \quad \forall\ w_h \in W_h \tag{21}$$

with

$$R_E(w_h) = \begin{cases} -\left[\!\left| \varepsilon \mathbf{n}_E \cdot \nabla w_h \right|\!\right]_E & \text{if } E \not\subset \partial\Omega, \\ g - \varepsilon \mathbf{n}_E \cdot \nabla w_h & \text{if } E \subset \Gamma^N, \\ 0 & \text{if } E \subset \Gamma^D, \end{cases}$$

and

$$\alpha_K = \min\left\{\mathrm{diam}(K)\varepsilon^{-1/2}, c_0^{-1/2}\right\}, \quad \alpha_E = \min\left\{\mathrm{diam}(E)\varepsilon^{-1/2}, c_0^{-1/2}\right\}.$$

Here, $\mathrm{diam}(K)$ and $\mathrm{diam}(E)$ denote the diameters of the mesh cell K and the face E, respectively, $\mathbf{n}_E$ is a unit normal on E, and c_0 is defined in (2). The jump of a function across the face E is denoted by $\left[\!\left|\cdot\right|\!\right]_E$. This error estimator is robust in a norm that is a sum of the standard energy norm and a dual norm of the convective derivative, see [34].

The right-hand side of the adjoint problem for the functional (21) is given by

$$
\begin{aligned}
&\langle D\tilde{I}_h(u_h(y_h)), v_h\rangle \\
&= \sum_{K\in\mathcal{T}_h} 2\alpha_K^2 \left(-\varepsilon\Delta\tilde{u}_h(y_h) + \mathbf{b}\cdot\nabla\tilde{u}_h(y_h) + c\tilde{u}_h(y_h) - f, -\varepsilon\Delta v_h + \mathbf{b}\cdot\nabla v_h + cv_h\right)_K \\
&\quad + \sum_{E\subset\partial K} 2\varepsilon^{-1/2}\alpha_E \left(R_E(\tilde{u}_h(y_h)), \tilde{R}_E(\tilde{v}_h)\right)_E,
\end{aligned}
$$

where $\tilde{R}_E(\tilde{v}_h)$ is defined by neglecting g in $R_E(\tilde{v}_h)$.

In the studies of Example 5.2, one could observe that the global errors were dominated by the local errors that occur in the approximation of the layers at the Dirichlet boundary. These local errors could not be significantly reduced by optimizing the stabilization parameter. As the algorithm concentrates on the reduction of the dominating errors, the errors in mesh cells away from the Dirichlet boundary were also not reduced notably. For this reason, an error indicator that excludes the mesh cells at the Dirichlet boundary will be considered, too. Further, we could observe that the influence of the residuals on the edges in (21) is negligible. One obtains practically the same results with and without using these terms. Thus, besides (21), the error indicator

$$
\begin{aligned}
&I_h(w_h) = \\
&\sum_{K\in\mathcal{T}_h,\overline{K}\cap\overline{\Gamma^D}=\emptyset} \alpha_K^2 \,\| -\varepsilon\,\Delta w_h + \mathbf{b}\cdot\nabla w_h + c\,w_h - f\|_{0,K}^2 \quad \forall\, w_h\in W_h
\end{aligned}
\tag{22}
$$

will be considered. Note, the mesh cells at the Dirichlet boundary do not contribute to the error indicator, but the stabilization parameter in these cells is still included into the optimization process.

The numerical studies will consider a standard example, defined on the unit square, that is often used for the evaluation of stabilized methods, and an example in a more complicated domain that gripped some attraction in the past years. Both examples have the properties $\mathrm{div}\mathbf{b} = 0$, $c = 0$, such that the upper bound (9) for the stabilization parameter applies.

Example 6.1 *Example with interior and exponential boundary layers.* This example was proposed in [17]. It is given by $\Omega = (0,1)^2$, $\Gamma^D = \partial\Omega$, with the data $\varepsilon = 10^{-8}$, $\mathbf{b} = (\cos(-\pi/3), \sin(-\pi/3))^T$, $c = 0$, $f = 0$, and

$$
u_b(x,y) = \begin{cases} 0 & \text{for } x = 1 \text{ or } y \le 0.7, \\ 1 & \text{else,} \end{cases}
$$

see Fig. 8 for the solution.

The simulations were performed on the grids given in Fig. 1. For shortness of presentation, only selected results are shown in Figs. 9 – 11. We could

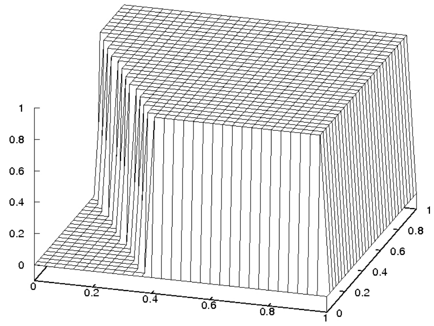

Fig. 8. Solution of Example 6.1.

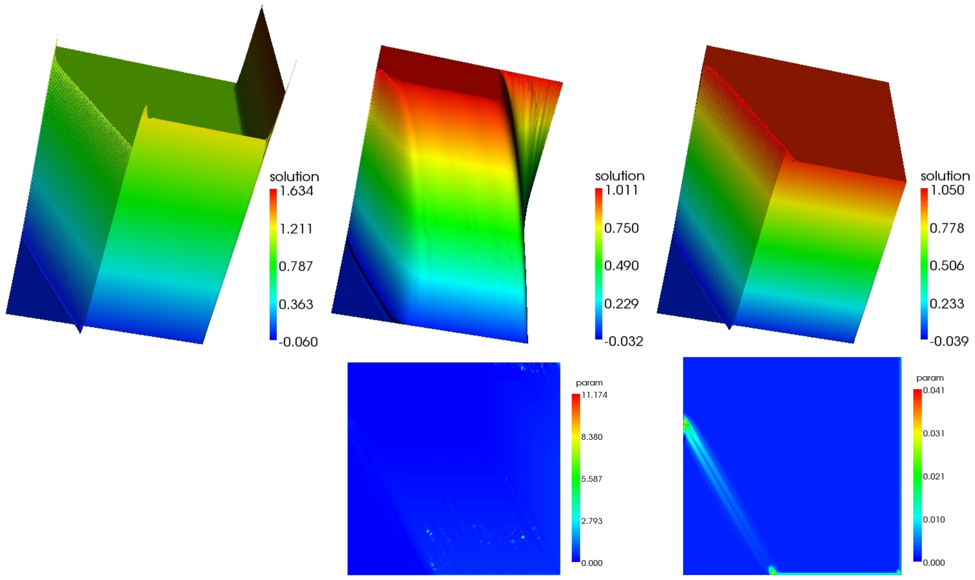

Fig. 9. Example 6.1: P_1, level 8, standard parameter (7) $y_h = 1.4298e-3$, minimization of (21), and minimization of (22), left to right.

observe that the principal behavior for P_k and Q_k finite elements, with the same k, was always similar. In all cases it can be seen that the minimization of the error estimator (21) leads to large values of the stabilization parameter and often to an extreme smearing of the layers. Minimizing (22) improves the solution significantly for the P_1 finite element, Fig. 9. The spurious oscillations are almost removed and the smearing of the layers is small. This is achieved by increasing the stabilization parameter in the regions of the interior layer and the boundary layer at $y = 0$. For the P_2 finite element, the minimization of (22) reduces the spurious oscillations somewhat but a substantially better solution than with the standard parameter choice is not obtained, Fig. 10. The boundary layer at $y = 0$ is somewhat smeared. A very large parameter is proposed at the position where the interior layer meets the boundary layer at the outflow boundary. In contrast to the quadratic finite element, the spurious oscillations are considerably reduced for the Q_3 finite element, Fig. 11, however the interior layer is greatly smeared. The minimization of (22) for Q_3 leads to a large stabilization parameter at the steep gradient of the boundary condition

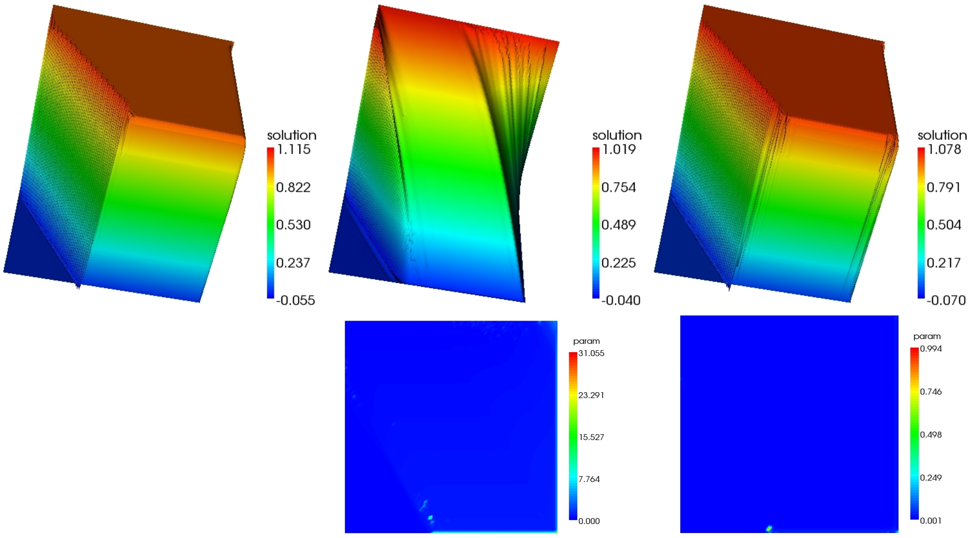

Fig. 10. Example 6.1: P_2, level 7, standard parameter (7) $y_h = 1.4298e-3$, minimization of (21), and minimization of (22), left to right.

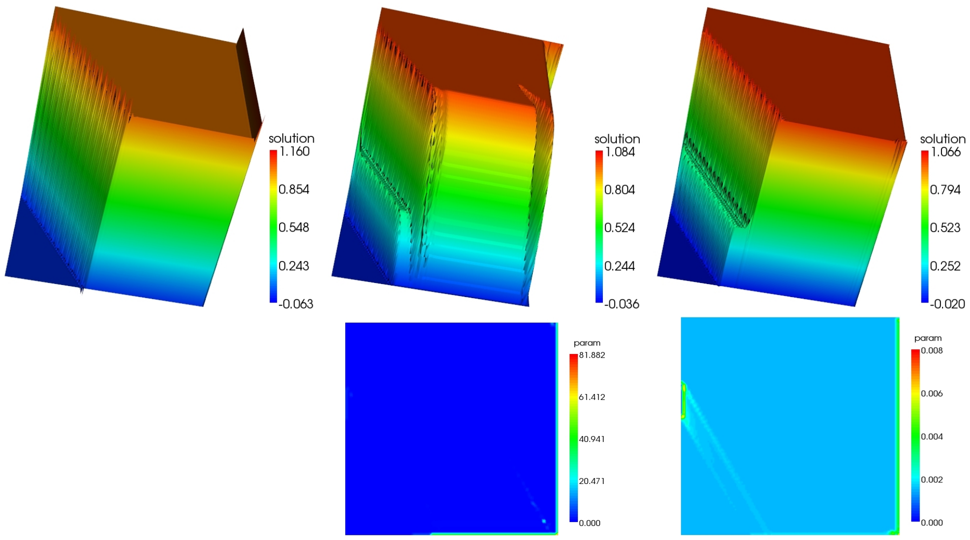

Fig. 11. Example 6.1: Q_3, level 7, standard parameter (7) $y_h = 1.5035e-3$, minimization of (21), and minimization of (22), left to right.

at the left inlet boundary. Similar results as presented here were obtained on a triangular grid where the diagonals are directed from top left to bottom right.

The principal effects of applying a stabilization parameter that minimizes the error estimator (21) and the indicator (22) are apparent: spurious oscillations are reduced and layers are smeared. Minimizing (21) leads obviously to too much smearing. A clear improvement of the solution, compared with the standard parameter choice, is achieved for the minimization of (22) using first order finite elements.

Example 6.2 *The Hemker example.* This example was defined in [14]. The computations were performed with $\Omega = \{[-3,8]\times[-3,3]\}\setminus\{(x,y) : x^2+y^2 < 1\}$, $\varepsilon = 10^{-6}$, $\mathbf{b} = (1,0)$, and $c = f = 0$. At the inlet $x = -3$, a homogeneous Dirichlet boundary condition is prescribed, at the circle there is $u = 1$, and on all other boundaries, homogeneous Neumann conditions are given.

This example attracted recently some interest, [11,32], since it is considered to be closer to situations arising in applications than many usual test examples. It can be interpreted as a model of heat transfer from a hot column in the direction of the convection. The initial grid (level 0) is shown in Fig. 12. Isoparametric finite elements were used to approximate the curved boundary. Results are presented for the Q_1 finite element on level 5 (189 536 d.o.f.), for the Q_2 finite element on level 4 (189 536 d.o.f.), and for the Q_3 finite element on level 4 as well (425 616 d.o.f.).

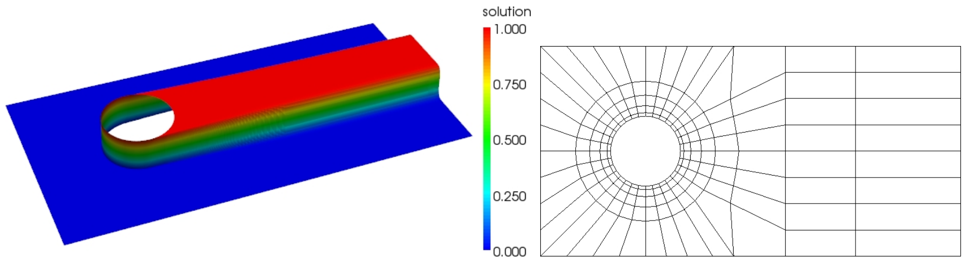

Fig. 12. Solution and initial grid for Example 6.2.

Results obtained with the SUPG method based on the parameter choice (7) and the methods based on minimizing the error estimates (21) and (22), respectively, are presented in Figs. 13 – 15. Note that for visualization purposes, the finite element solutions were restricted to a Q_1 function, such that the solutions for higher order finite elements are smoother than they look in the pictures. Fig. 13 shows that the minimization of (21) reduces again most of the spurious oscillations, but the layer in front of the circle is smeared considerably. Similar results were obtained with the higher order finite elements, which are not shown for shortness of presentation. Minimizing (22) increases the stabilization parameter in the layers starting at the circle. For the Q_1 and Q_3 finite elements, the negative spurious oscillations at the circle are reduced to some extent, Figs. 13 and 15. Concerning the Q_2 finite element, the solutions obtained with (7) and the minimization of (21) are rather similar. Both results correspond with the observations of Example 6.1 concerning the effect of minimizing (22) for finite elements with different polynomial degrees.

For the minimization of (22) and the Q_1 finite element, the effect of using different initial values for the stabilization parameter was studied. Results are presented in Fig. 16, which should be compared with the results on the bottom of Fig. 13. The first two studies used as starting values a multiple of the standard choice (7), more precisely, a third of the standard choice and three times the standard choice. It can be observed that the first choice leads to large values of the stabilization parameter in front of the circle, which

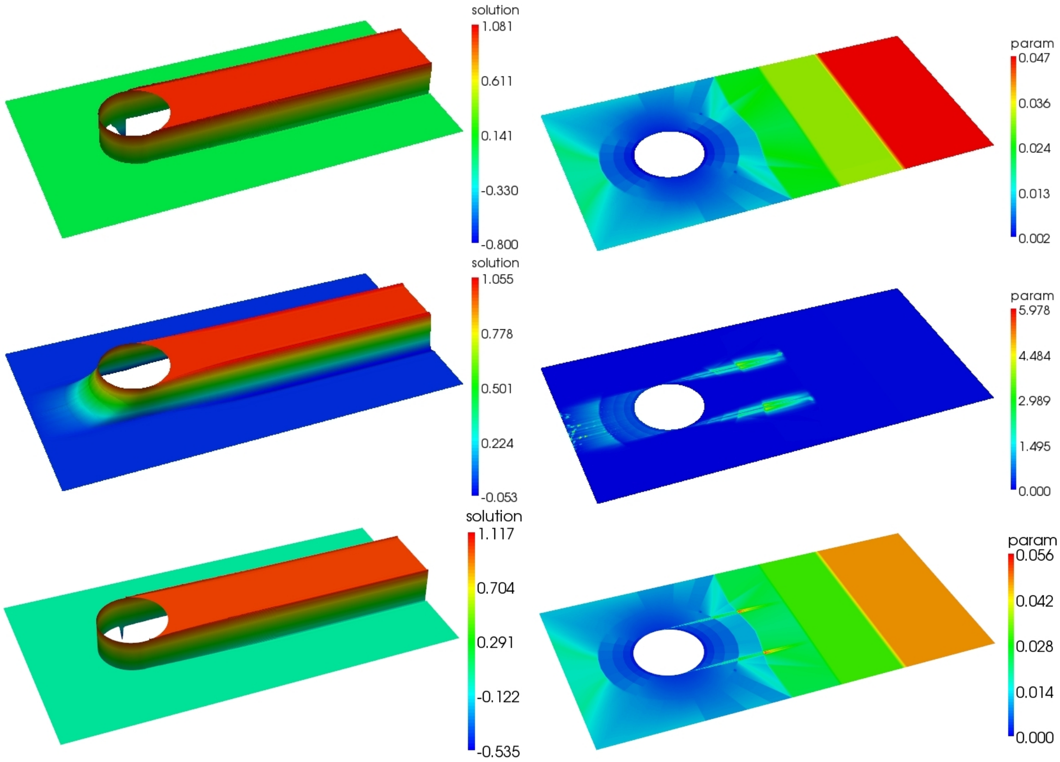

Fig. 13. Example 6.2: Q_1, level 5, standard parameter (7), minimization of (21), and minimization of (22), top to bottom.

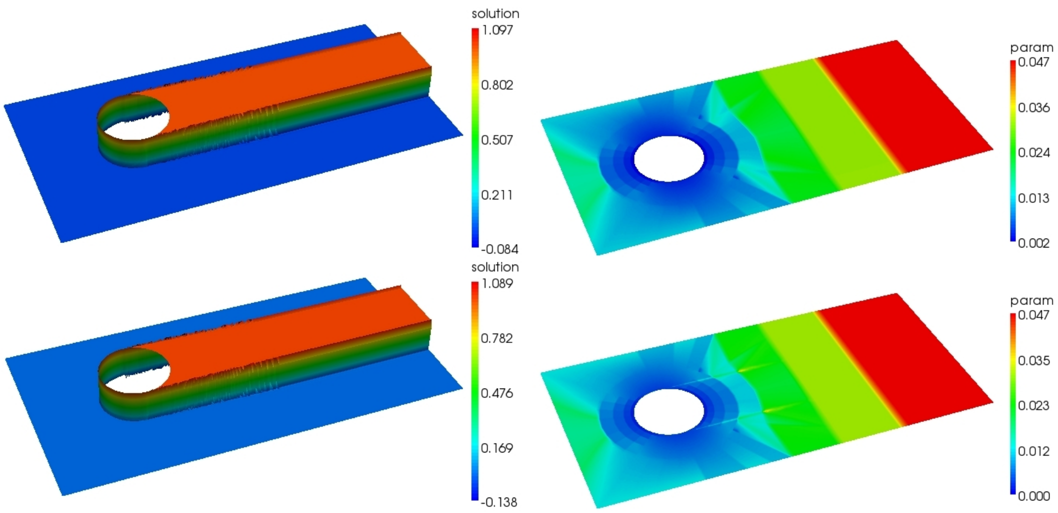

Fig. 14. Example 6.2: Q_2, level 4, standard parameter (7) and minimization of (22), top to bottom.

results in a smeared solution in this region. The computed results with the second choice look very similar to the results from Fig. 13. In both cases, the minimization of (22) leads to an increase of the stabilization parameter along the interior layers, starting from the circle. The parameter in the smooth regions of the solution does not change much during the minimization process.

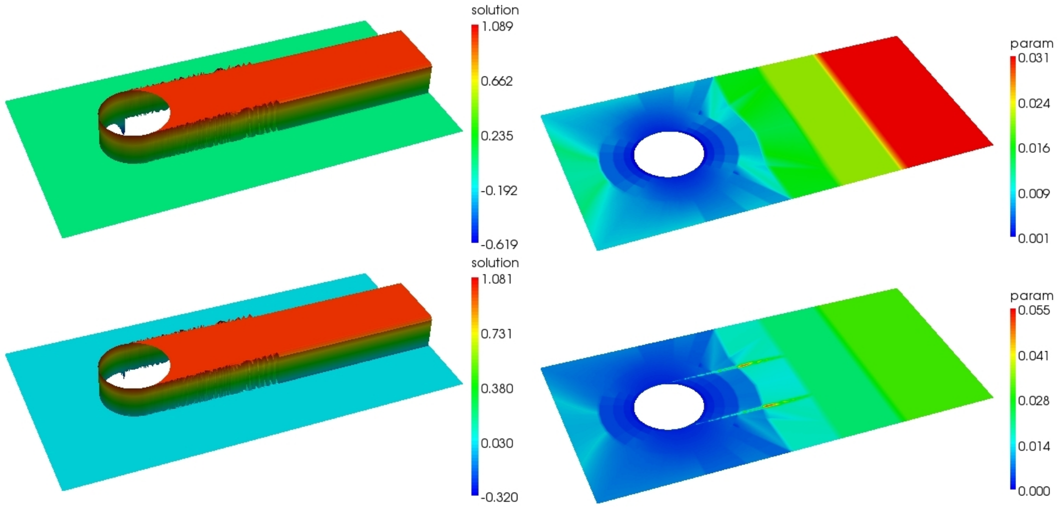

Fig. 15. Example 6.2: Q_3, level 4, standard parameter (7) and minimization of (22), top to bottom.

The local strong residual is very small in these parts and so the variation of the parameter has only little influence on the solution and thus on the error indicator. This means, (22) is rather flat in a neighborhood of its minimum, which might lead to an inefficient behavior of the steepest descent method (19).

The third an fourth study started with a constant parameter. Using the large parameter $y_h|_K = 0.1$, the minimization leads to an increase of the stabilization parameter in the same regions as in the previous simulations. Simultaneously, the parameter was decreased directly in front of the circle and then increased into the direction of the inlet. Finally, a rather good solution is computed. Starting with the very small parameter $y_h|_K = 10^{-5}$, a large stabilization parameter is proposed at the inlet. Obviously, the stabilization parameter is increased in regions were it is needed, since the computed solution is comparable to the solution obtained with the large initial value. Only small oscillations from the circle against the direction of the convection can be seen. We could learn in further studies that this rather favorable behavior cannot be observed if the initial values of the parameter are too small compared with the standard values.

Some general remarks on the efficiency of the steepest descent method (19) will be given last. The number of iterations, until one of the stopping criteria was fulfilled, varied very much, depending above all on the example and the degree of the finite element. Sometimes, a few iterations (≤ 10) were sufficient, sometimes the minimization took several thousands of iterations. As mentioned already above, the values of the stabilization parameter have very little effect on the solution in smooth regions and hence varying them has also little influence on the target functional. This seems to be one reason why (19) is sometimes rather inefficient. To get first impressions on the benefits and

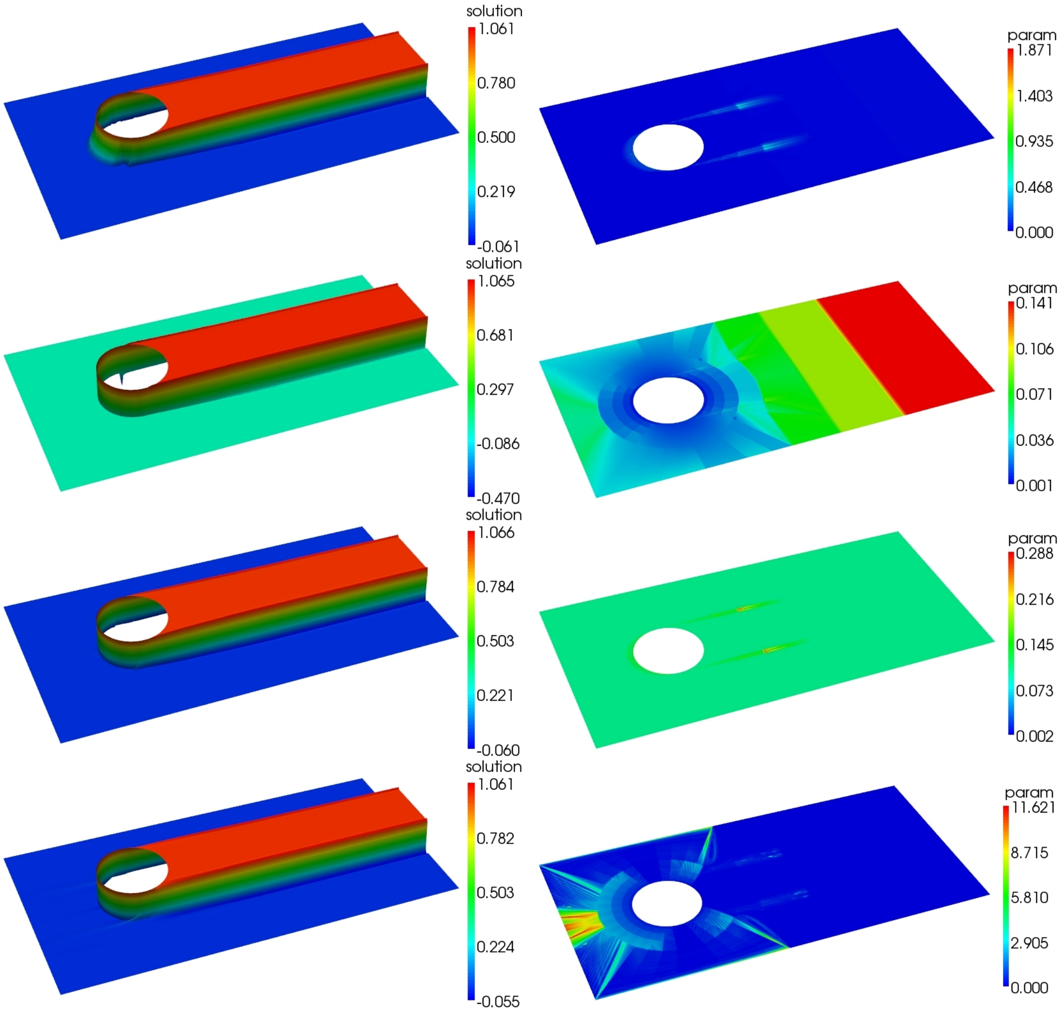

Fig. 16. Example 6.2: Q_1, level 5, starting with: one third of standard parameter (7), three times the standard parameter, $y_h|_K = 0.1$, and $y_h|_K = 10^{-5}$, top to bottom.

difficulties of the basic approach for stabilization parameter optimization, the use of the current method was sufficient. However, for the a posteriori stabilization parameter choice to become attractive in applications, the efficiency of the iterative procedure has to be improved certainly.

7 Summary and outlook

This paper presented a general framework for optimizing the parameter in stabilized finite element methods for convection-diffusion problems. The optimization is based on minimizing a target functional that indicates the quality of the computed solution. A damped steepest descent method is used to solve the arising constrained optimization problem. Key of the algorithm is the efficient evaluation of the derivative of the target functional with respect to the stabilization parameter that utilizes the solution of an appropriate adjoint problem. Benefits and difficulties of this basic approach were studied exemplarily at the SUPG finite element method and the minimization of a residual-based error estimator and an error indicator.

Important next steps in the exploration and improvement of the parameter optimization are as follows:

- It is not clear if the introduction of diffusion in streamline direction only, as in the SUPG method, suffices to obtain satisfactory numerical solutions. Some diffusion orthogonal to the streamlines might be necessary, as it is done by the SOLD methods. The new aspect in the application of the general framework to SOLD methods consists in the optimization of two stabilization parameters.
- The computed solution can be only as good as its quality is measured by the target functional. It could be already observed that a residual-based a posteriori error estimator has to be modified, using (22) instead of (21), to obtain reasonable solutions. Possible other functionals which will be studied include, e.g., error estimators that are based on the DWR approach, [1,2].
- Algorithmic improvements are necessary. These include, e.g., increasing the efficiency of the iterative method for solving the optimization problem and the use of more restrictive upper bounds for the stabilization parameter than proposed by the analysis.

A medium term goal consists in the consideration of time-dependent problems.

References

[1] W. Bangerth and R. Rannacher. *Adaptive finite element methods for differential equations.* Lectures in Mathematics, ETH Zürich. Birkhäuser Basel, 2003.

[2] R. Becker and R. Rannacher. An optimal control approach to a posteriori error estimation in finite element methods. In A. Iserles, editor, *Acta Numerica*, pages 1 – 102. Cambridge University Press, 2004.

[3] A.N. Brooks and T.J.R. Hughes. Streamline upwind/Petrov–Galerkin formulations for convection dominated flows with particular emphasis on the incompressible Navier–Stokes equations. *Comput. Methods Appl. Mech. Engrg.*, 32:199 – 259, 1982.

[4] P.G. Ciarlet. Basic error estimates for elliptic problems. In P.G. Ciarlet and J.L. Lions, editors, *Handbook of Numerical Analysis, v. 2 – Finite Element Methods (pt. 1)*, pages 17–351. North-Holland, Amsterdam, 1991.

[5] R. Codina, E. Oñate, and M. Cervera. The intrinsic time for the streamline upwind/Petrov–Galerkin formulation using quadratic elements. *Comput.*

Methods Appl. Mech. Engrg., 94:239 – 262, 1992.

[6] C. Führer and R. Rannacher. An adaptive streamline-diffusion finite element method for hyperbolic conservation laws. *East–West J. Numer. Math.*, 5:145 – 162, 1997.

[7] A. C. Galeão, R. C. Almeida, S. M. C. Malta, and A. F. D. Loula. Finite element analysis of convection dominated reaction–diffusion problems. *Appl. Numer. Math.*, 48:205–222, 2004.

[8] M. Germano, U. Piomelli, P. Moin, and W. Cabot. A dynamic subgrid-scale eddy viscosity model. *Phys. Fluids A*, 3:1760 – 1765, 1991.

[9] M. B. Giles and N. A. Pierce. An introduction to the adjoint approach to design. *Flow, Turbulence and Combustion*, 65:393–415, 2000.

[10] J.-L. Guermond. Stabilization of Galerkin approximations of transport equations by subgrid modeling. *M2AN*, 33:1293 – 1316, 1999.

[11] H. Han, Z. Huang, and R.B. Kellogg. A tailored finite point method for a singular perturbation problem on an unbounded domain. *J. Sci. Comput.*, 36:243 – 261, 2008.

[12] I. Harari and T.J.R. Hughes. What are c and h?: Inequalities for the analysis and design of finite element methods. *Comput. Methods Appl. Mech. Engrg.*, 97:157 – 192, 1992.

[13] F.K. Hebeker and R. Rannacher. An adaptive finite element method for unsteady convection-dominated flows with stiff source terms. *SIAM J. Sci. Comput.*, 21:799 – 818, 1999.

[14] W.P. Hemker. A singularly perturbed model problem for numerical computation. *J. Comp. Appl. Math.*, 76:277 – 285, 1996.

[15] T.J.R. Hughes. Multiscale phenomena: Green's functions, the Dirichlet-to-Neumann formulation, subgrid-scale models, bubbles and the origin of stabilized methods. *Comput. Methods Appl. Mech. Engrg.*, 127:387 – 401, 1995.

[16] T.J.R. Hughes and A.N. Brooks. A multidimensional upwind scheme with no crosswind diffusion. In T.J.R. Hughes, editor, *Finite Element Methods for Convection Dominated Flows, AMD vol.34*, pages 19 – 35. ASME, New York, 1979.

[17] T.J.R. Hughes, M. Mallet, and A. Mizukami. A new finite element formulation for computational fluid dynamics: II. beyond SUPG. *Comput. Methods Appl. Mech. Engrg.*, 54:341 – 355, 1986.

[18] V. John. A numerical study of a posteriori error estimators for convection-diffusion equations. *Comput. Methods Appl. Mech. Engrg.*, 190:757 – 781, 2000.

[19] V. John. *Large Eddy Simulation of Turbulent Incompressible Flows. Analytical and Numerical Results for a Class of LES Models*, volume 34 of *Lecture Notes in Computational Science and Engineering*. Springer–Verlag Berlin, Heidelberg, New York, 2004.

[20] V. John and S. Kaya. A finite element variational multiscale method for the Navier–Stokes equations. *SIAM J. Sci. Comp.*, 26:1485 – 1503, 2005.

[21] V. John and A. Kindl. A variational multiscale method for turbulent flow simulation with adaptive large scale space. *J. Comput. Phys.*, 229:301 – 312, 2010.

[22] V. John and P. Knobloch. A comparison of spurious oscillations at layers diminishing (SOLD) methods for convection–diffusion equations: Part I – a review. *Comput. Methods Appl. Mech. Engrg.*, 196:2197 – 2215, 2007.

[23] V. John and P. Knobloch. A comparison of spurious oscillations at layers diminishing (SOLD) methods for convection-diffusion equations: Part II – analysis for P_1 and Q_1 finite elements. *Comput. Methods Appl. Mech. Engrg.*, 197:1997 – 2014, 2008.

[24] V. John and G. Matthies. MooNMD - a program package based on mapped finite element methods. *Comput. Visual. Sci.*, 6:163 – 170, 2004.

[25] V. John, J.M. Maubach, and L. Tobiska. Nonconforming streamline-diffusion-finite-element-methods for convection-diffusion problems. *Numer. Math.*, 78:165 – 188, 1997.

[26] V. John and E. Schmeyer. Stabilized finite element methods for time-dependent convection-diffusion-reaction equations. *Comput. Methods Appl. Mech. Engrg.*, 198:475 – 494, 2008.

[27] O.A. Ladyzhenskaya. New equations for the description of motion of viscous incompressible fluids and solvability in the large of boundary value problems for them. *Proc. Steklov Inst. Math.*, 102:95 – 118, 1967.

[28] D.K. Lilly. A proposed modification of the Germano subgrid-scale closure method. *Phys. Fluids A*, 4:633 – 635, 1992.

[29] H.-G. Roos, M. Stynes, and L. Tobiska. *Robust Numerical Methods for Singularly Perturbed Differential Equations. Convection–Diffusion–Reaction and Flow Problems. 2nd ed.* Springer-Verlag, Berlin, 2008.

[30] R. Schneider. *Applications of the discrete adjoint method in computational fluid dynamics.* PhD thesis, University of Leeds, School of Computing, 2006.

[31] J.S. Smagorinsky. General circulation experiments with the primitive equations. *Mon. Weather Review*, 91:99 – 164, 1963.

[32] P. Sun, L., and J. Xu. Numerical studies of adaptive finite element methods for two dimensional convection-dominated problems. *J. Sci. Comput.*, 43:24 – 43, 2010.

[33] F. Tröltzsch. *Optimale Steuerung partieller Differentialgleichungen - Theorie, Verfahren und Anwendungen.* Vieweg+Teubner Verlag, 2nd edition, 2009.

[34] R. Verfürth. Robust a posteriori error estimates for stationary convection-diffusion equations. *SIAM J. Numer. Anal.*, 43:1766 – 1782, 2005.